Estimation and validation of actual evapotranspiration for wheat crop using SEBAL model over Hisar district, Haryana, India

Anju Bala[1,3,*], Prakashkiran S. Pawar[2], Anil Kumar Misra[3] and Kishan Singh Rawat[4]

[1]Department of Civil Engineering, K. R. Mangalam University, Gurgaon 122 001, India
[2]The Energy and Resources Institute, New Delhi 110 003, India
[3]Department of Civil and Environmental Engineering, The Northcap University, Gurgaon 122 017, India
[4]Centre for Remote Sensing and Geo-Informatics, Sathyabama University, Chennai 600 119, India

Evapotranspiration (ET) is one of the complex, but essential components of the hydrologic cycle. Advances in remote sensing (RS) and geographical information systems (GIS) have enabled us to estimate ET spatially. In the present study, both, RS and GIS tools have been utilized to estimate the actual crop ET by surface energy balance algorithm for land (SEBAL) model using high spatial resolution satellite image Landsat7 ETM+ for Hisar district, Haryana in north India. Previously calibrated and validated SEBAL model with lysimeter data within the same agro-climatic zone were used in the study. Derived actual ET from lysimeter data validated SEBAL method was again validated using Penman–Montieth (PM) method for the study area located in the same agro-climatic zone. Based on the primary and secondary data analysis, it can be inferred that SEBAL ET is the best spatial ET estimation model for Hisar district or regions having similar agro-climatic conditions. Validation of SEBAL ET with ground-observed lysimeter data showed high coefficient of correlation ($R^2 = 0.91$). Validation using the PM method also showed high coefficient of correlation ($R^2 = 0.835$). Other statistical parameters (RMSE = 0.583, NRMSE = 0.236) also showed good agreement between actual SEBAL ET_c and PM ET_c (crop evapotranspiration). It was also found that any prior knowledge about the crops, their types and cropping seasons is not required for the estimation of actual ET by SEBAL model.

Keywords: Energy balance algorithm, evapotranspiration, ground truthing, remote sensing, wheat.

OVER the last few decades with the reduction of water resources, India is facing critical problems with industrial and agricultural growth being impacted[1]. In agriculture, water requirements are associated with irrigation water use. Prediction of irrigation water demand involves computation of many water balance factors, and evapotranspiration (ET) is one of its major components. ET is the combined loss of water from the soil as well as plants and it is a crucial component of the hydrologic cycle. At the same time, ET depends upon several factors and is difficult to calculate precisely. Remote sensing (RS) techniques are emerging to solve this problem by providing reliable algorithms. Several models have been developed to derive ET fluxes like surface energy balance algorithm for land (SEBAL)[2], simplified surface energy balance index (S-SEBI)[3], two-source energy balance (TSEB)[4] and surface energy balance system (SEBS)[5]. SEBAL is one of the best models to estimate spatial ET because it calculates the fluxes independently from land cover and can handle thermal infrared images at resolutions between a few metres and several kilometres[6]. Due to these major advantages of this surface energy balance model, it was adopted for the spatial estimation of ET in Hisar district, Haryana, India. SEBAL model was used in the present study which was already validated using lysimeter data from a nearby location, i.e. Water Technology Centre, Indian Agricultural Research Institute (IARI), New Delhi[7]. The reference crop ET can be accurately calculated by Penman–Monteith (PM) model (FAO Standard method; FAO-56 guidelines) which is most common and practical approach widely used for estimating crop water requirement[8]. To calculate actual ET crop coefficient approach is implemented; crop coefficient further depends upon greenness, crop cover and leaf area index. To differentiate the crop from reference surface[9], K_c is a key variable. It not only differs in different ecological systems or ecosystems, but also with variation in environment[10,11].

In the SEBAL model, within each analysed satellite image automatic internal calibration is done which decreases the biasness in estimation of surface roughness and aerodynamic stability correction. This calibration also reduces the requirement for atmospheric correction of surface temperature (T_s) or reflectance (albedo) measurements using radiative transfer models[12]. The other advantage is that it calculates actual ET instead of potential ET. Owing to all these facts, the SEBAL model is extensively used for various agricultural crops as well as in a variety of ecosystems and climates, provided it is validated in that particular agro-climatic zone[13].

Among various problems in ET estimation, validation is a major one, particularly because of both the scaling and advection effects[14]. Such issues may be resolved by developing various validation methods, which may include comparison of ET derived from RS and ground-based measurements over the same location. Thus the present study was carried out with the objective of spatial ET estimation using the SEBAL model, which was already validated/tested in the same agro-climatic zone[7] using Landsat7 ETM+ data for Hisar district. Another objective was to validate the SEBAL model by ground truthing of the study area using PM model according to FAO 56 guidelines[8] and using locally developed crop coefficients.

*For correspondence. (e-mail: anjukathuria@yahoo.com)

Hisar district is situated between 28°56′00″–29°38′30″N lat. and 75°21′12″–76°18′12″E long. The normal annual rainfall of the district is 330 mm, which is unevenly distributed over the area. Wheat, mustard and gram are the three major crops of *rabi* season, which are evenly spread throughout the district and occupy around 2378.29 ('000 ha) area. The district covers an area of 3983.00 sq. km. Figure 1 shows a map of the study area.

For validation of SEBAL ET, the ground-observed lysimeter data were taken from a nearby location, i.e. at Water Technology Centre (WTC) farm of IARI, New Delhi and all the field experiments were conducted during 2010–11. The experimental data were used for validation of the SEBAL model and this validated model was used for spatial estimation of ET at another location in the same agro-climatic zone. Detailed procedure and other information are available in Bala *et al.*[7].

Using the SEBAL model, ET was estimated for the study area for five crop years of wheat crop seasons, viz. 2004–05, 2005–06, 2007–08, 2012–13 and 2013–14. The imageries were taken for at least three cloud-free dates for each year at three different stages of crop growth, viz. (i) early growth stage (December/January), (ii) middle stage (February), and (iii) at full growth stage (March) of wheat crop. Table 1 lists the Landsat images used for ET estimation by SEBAL method. The satellite data used in this study were Landsat7 ETM+ images. All these images were geometrically and radiometrically corrected and geo-registered.

For further validation, ground truthing survey of Hisar district was done. Wheat is the major crop in the study area and it occupies maximum area[15]. Ground truthing survey was done to identify wheat fields in the study area with high precision GARMIN GPS (global positioning system), during 2012–13 and 2013–14 in five different villages in the study area (Table 2). Wheat crop fields of size 2 ha more were selected to avoid image resolution issues (Figure 2). Wheat field coordinates (Table 2) were superimposed on ET imageries of 2012–13 and 2013–14 crop seasons to identify wheat fields.

To calculate the crop coefficients (K_c), field data in form of standard date of sowing, days passed after sowing, plant height, plant width, crop growth stage, etc. were collected for selected fields in the study area. Daily meteorological data were taken from the Regional

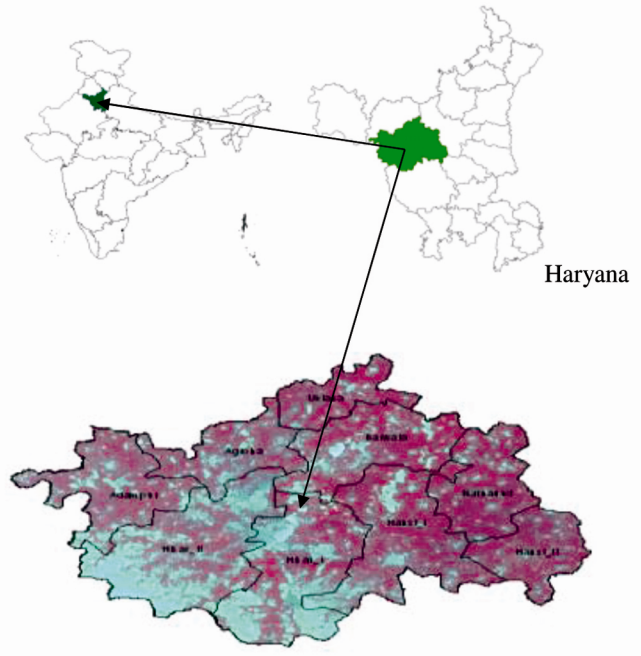

Figure 1. Location map of the study area.

Table 1. Description of acquired remote sensing data

Date of data acquired	Row/path	Sensor
30 January 2005	147/40	Landsat7 ETM+
14 February 2005	147/40	Landsat7 ETM+
3 March 2005	147/40	Landsat7 ETM+
16 December 2005	147/40	Landsat7 ETM+
6 March 2006	147/40	Landsat7 ETM+
22 March 2006	147/40	Landsat7 ETM+
22 December 2007	147/40	Landsat7 ETM+
23 January 2008	147/40	Landsat7 ETM+
24 February 2008	147/40	Landsat7 ETM+
19 December 2012	147/40	Landsat7 ETM+
9 March 2013	147/40	Landsat7 ETM+
25 March 2013	147/40	Landsat7 ETM+
6 December 2013	147/40	Landsat7 ETM+
7 January 2014	147/40	Landsat7 ETM+
12 March 2014	147/40	Landsat7 ETM+

Figure 2. Zoomed image of wheat field coordinates superimposed on the satellite image.

Table 2. Coordinates of pure wheat-dominated areas

Village	Longitude	Latitude
Durjanpur	75°38′44.50″	29°14′16.06″
Neoli Khurad	75°36′39.54″	29°12′51.12″
Kajla	75°36′49.47″	29°14′14.38″
Malapar	75°35′14.52″	29°13′33.46″
Jakod Khera	75°34′4.20″	29°12′47.34″

Meteorological Station of India Meteorological Department (IMD) at Chandigarh. Meteorological data, viz. temperature (minimum and maximum), relative humidity (minimum, maximum and average), wind speed, sunshine hours and precipitation were used to calculate reference evapotranspiration (ET_0) by PM method according to FAO-56 guidelines using CROPWAT 8.0 (software developed by FAO).

SEBAL is an image-processing model comprised of more than 25 computational steps that calculate actual ET as a residual term of surface energy balance at the time of satellite overpass. Bastiaansen *et al.*[6] also have provided the following energy balance equation

$$\mathrm{ET} = R_\mathrm{n} - H - G_0, \tag{1}$$

where ET is the latent heat flux associated with evaporation of water from the soil and from vegetation, R_n the net radiation absorbed at the land surface, H the sensible heat flux to warm or cool the atmosphere, and G_0 is the soil heat flux to warm or cool the soil, all expressed in Wm^{-2}.

After acquiring satellite images using reflectance from visible, infrared and thermal bands, normalized difference vegetation index (NDVI), leaf area index (LAI), surface temperature and albedo maps were generated and then all the fluxes mentioned in eq. (1) were estimated[6,7]. By summing up long- and shortwave radiations, the net radiation was estimated. Soil heat flux was calculated using the following empirical equation of Bastiaanssen and Roebeling[16]

$$\frac{G_0}{R_\mathrm{n}} = \frac{(T_\mathrm{s} - 273.15)}{100\alpha}(0.32\alpha + 0.62\alpha^2)(1 - 0.98\mathrm{NDVI}^4), \tag{2}$$

where α is the average albedo, T_s is the surface temperature (K) and NDVI is the normalized vegetation index.

Sensible heat flux being a complex component was correctly solved using iteration procedure by developing empirical coefficients for each satellite image. Finally after estimating all the fluxes, actual ET was estimated by energy balance method on a pixel by pixel basis.

After incorporating the equations of aerodynamic and surface resistance in the original PM equation, then equation became FAO PM standard method[11], which is the most widely used and most accurate point ET estimation method

$$\mathrm{ET_o} = \frac{0.408\Delta(R_\mathrm{n} - G) + \gamma \frac{900}{T+273} u_2 (e_\mathrm{s} - e_\mathrm{a})}{\Delta + \gamma(1 + 0.34u_2)}, \tag{3}$$

where $\mathrm{ET_o}$ is the reference ET (mm day^{-1}), R_n the net radiation at the crop surface (MJ $\mathrm{m}^{-2}\,\mathrm{day}^{-1}$), G the soil heat flux density (MJ $\mathrm{m}^{-2}\,\mathrm{day}^{-1}$), T the mean daily air temperature at 2 m height (°C), u_2 the wind speed at 2 m height ($\mathrm{m\,s}^{-1}$), e_s the saturation vapour pressure ($\mathrm{kP_a}$), e_a the actual vapour pressure ($\mathrm{kP_a}$), $e_\mathrm{s} - e_\mathrm{a}$ the saturation vapour pressure deficit ($\mathrm{kP_a}$), Δ the slope vapour pressure curve ($\mathrm{kP_a\ °C^{-1}}$), and γ is the psychrometric constant ($\mathrm{kP_a\ °C^{-1}}$).

Using weather data mentioned above, ET_0 for the same dates of satellite images was estimated by PM method using CROPWAT 8.0.

The crop coefficients required to estimate actual ET for wheat crop were estimated by FAO recommended guidelines for local region (Hisar district). For each crop growth stage and each crop year, crop coefficient curves were developed. These curves were used to estimate the crop coefficient for the date of satellite image. Cross-checking of crop coefficients was also done by taking information of local standard practices. It was found that the developed crop coefficients are robust.

In Hisar district, wheat crop is grown usually in middle of November and harvested in the middle of April. Crop coefficients were found for all the growth stages, i.e. initial, mid and end stages. Using these values crop coefficient curves were plotted for each crop year. Figure 3 shows a typical crop coefficient curve for wheat crop during 2013–14 in Hisar district. The crop coefficient curves were used to estimate the crop coefficient for the date of satellite image. Average crop coefficients for the initial,

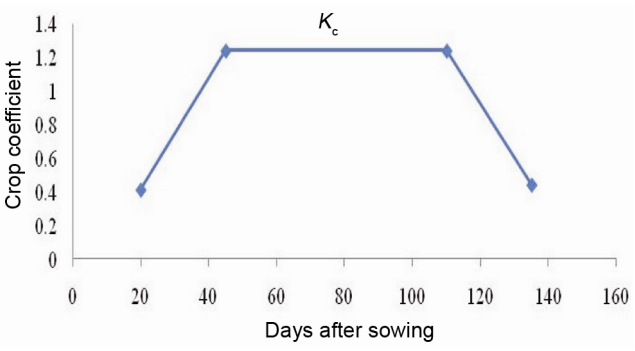

Figure 3. Crop coefficient curve.

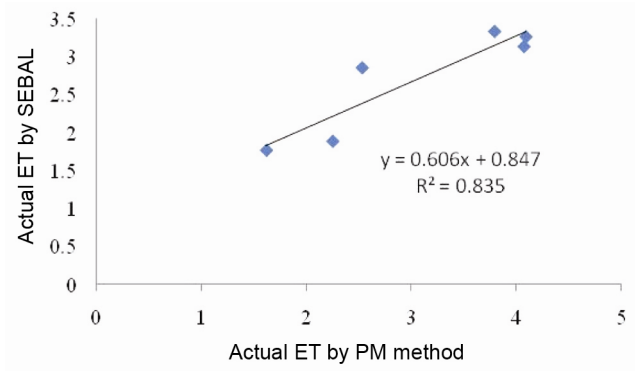

Figure 4. Correlation between SEBAL ET and PM ET at ground truthing points during crop seasons 2012–13 and 2013–14 in Hisar district, Haryana.

Table 3. Actual ET by SEBAL at ground truthing points in Hisar district, during crop seasons 2012–13 and 2013–14

19 December 2012	SEBAL_ET	6 December 2013	SEBAL_ET
Field 1	2.35	Field 1	1.68
Filed 2	2.04	Filed 2	2.07
Field 3	1.92	Field 3	1.22
Filed 4	2.39	Filed 4	1.61
Field 5	2.55	Field 5	1.52
Average SEBAL ET_c	2.25	Average SEBAL ET_c	1.61
9 March 2013		7 January 2014	
Field 1	3.45	Field 1	2.87
Filed 2	3.89	Filed 2	2.07
Field 3	4.23	Field 3	3.14
Filed 4	3.69	Filed 4	2.15
Field 5	3.69	Field 5	2.41
Average SEBAL ET_c	3.79	Average SEBAL ET_c	2.53
25 March 2013		12 March 2014	
Field 1	4.12	Field 1	3.87
Filed 2	3.75	Filed 2	4.34
Field 3	4.04	Field 3	3.69
Filed 4	4.47	Filed 4	4.36
Field 5	3.97	Field 5	4.19
Average SEBAL ET_c	4.07	Average SEBAL ET_c	4.09

Table 4. Actual ET by Penman Monteith method/model at ground truthing points in Hisar district during crop seasons 2012–13 and 2013–14

Date	Reference ET	K_c	Actual ET by PM method
19 December 2012	2.27	0.83	1.88
9 March 2013	2.97	1.12	3.33
25 March 2013	4.54	0.69	3.13
6 December 2013	4.19	0.42	1.76
7 January 2014	2.32	1.23	2.85
12 March 2014	3.17	1.03	3.26

mid and end stage were around 0.43, 1.23 and 0.44 respectively.

Figure 4 provides an assessment of SEBAL ET based on Landsat7 ETM+ satellite images for 2012–2013 and 2013–14 with PM ET at fixed points. Table 3 lists the average of SEBAL ET values for five fields, while Table 4 lists the actual ET by PM method at the same dates and time of satellite images. The derived actual SEBAL ET_c using remote sensing data by SEBAL model and estimated actual ET using PM method using weather data by Cropwat8.0, both these actual ET values were compared using statistical tests. Statistical comparison (Figure 4) shows that SEBAL calculated ET_c has good coefficient of correlation ($R^2 = 0.835$) with PM calculated ET_c in the study area. All other statistical parameters (RMSE = 0.583, NRMSE = 0.236) also show good agreement between actual SEBAL ET_c and PM ET (Table 5).

After validation of SEBAL ET with ground-observed lysimeter data with high coefficient of correlation ($R^2 = 0.91$)[7] and with PM ET_c having coefficient of correlation ($R^2 = 0.835$), the SEBAL model was applied over 15 different dates'/years' Landsat7 ETM+ images for ET mapping of the study area during wheat cropping seasons.

The SEBAL ET estimation involves calculation of different vegetation indices, viz. NDVI, LAI and soil adjusted vegetation index (SAVI). Standard practice was employed to estimate spatial ET. Figure 5 shows a typical result for 12 March 2014 images for NDVI, LAI and SAVI respectively. Procedure to estimate ET also involves the estimation of other important components (albedo, net radiation, surface temperature, ground heat flux, latent heat flux and evaporative fraction) from the SEBAL model. Figure 6 shows these results for 12 March 2014. Using these parameters, spatial ET was estimated for the study area for five crop years (Figure 7). Table 6 shows the results of ET_{min}, ET_{max} and ET_{avg}.

Average ET is found from the histogram of ET values in the image and it is the value of ET with maximum number of pixels in the image. Wheat fields are maximum in number in the study region, ET_{avg} represents the average ET values of wheat crop for the date of image. It was found that average estimated ET varies from 1.14 to 2.0 mm/day at early growth stage, 2.5 to 4 mm/day at middle growth stage and 3.0 to 4.5 mm/day at full growth stage of crop in Hisar district. Actual ET varies spatially with different vegetation cover, land-use practices and different types of land management practices even in the same climatic and meteorological conditions. This is shown by the range of actual ET values at different stages. ET_{min} is the lower value of ET in the area of lower moisture availability in the study area; due to this energy transformation in the context of sensible heat exchange is less. ET_{max} is ET from the area with water bodies or fields with well irrigation. Here ET is controlled by the

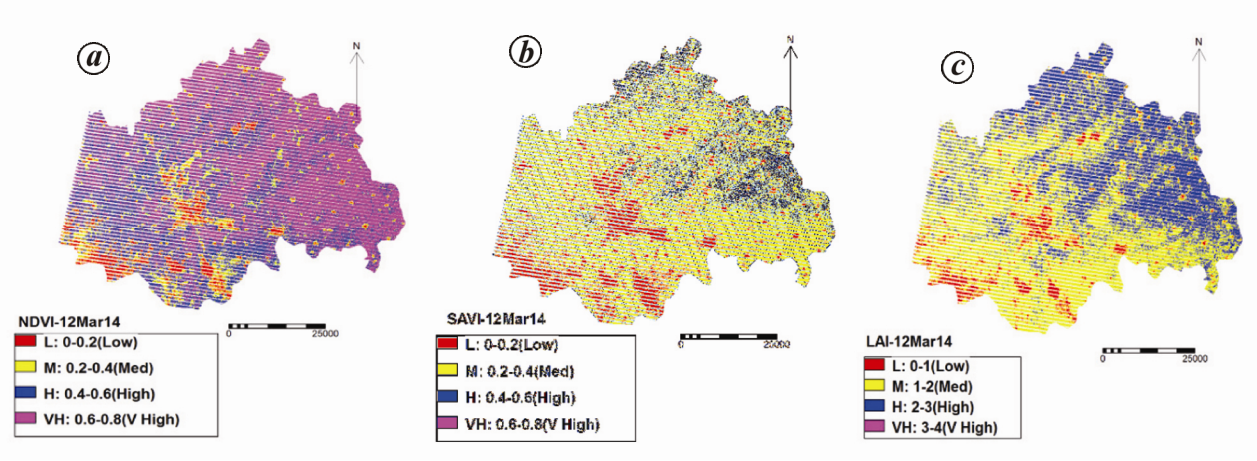

Figure 5. ***a***, Normalized difference vegetation index; ***b***, Soil-adjusted vegetation index; ***c***, Leaf area index.

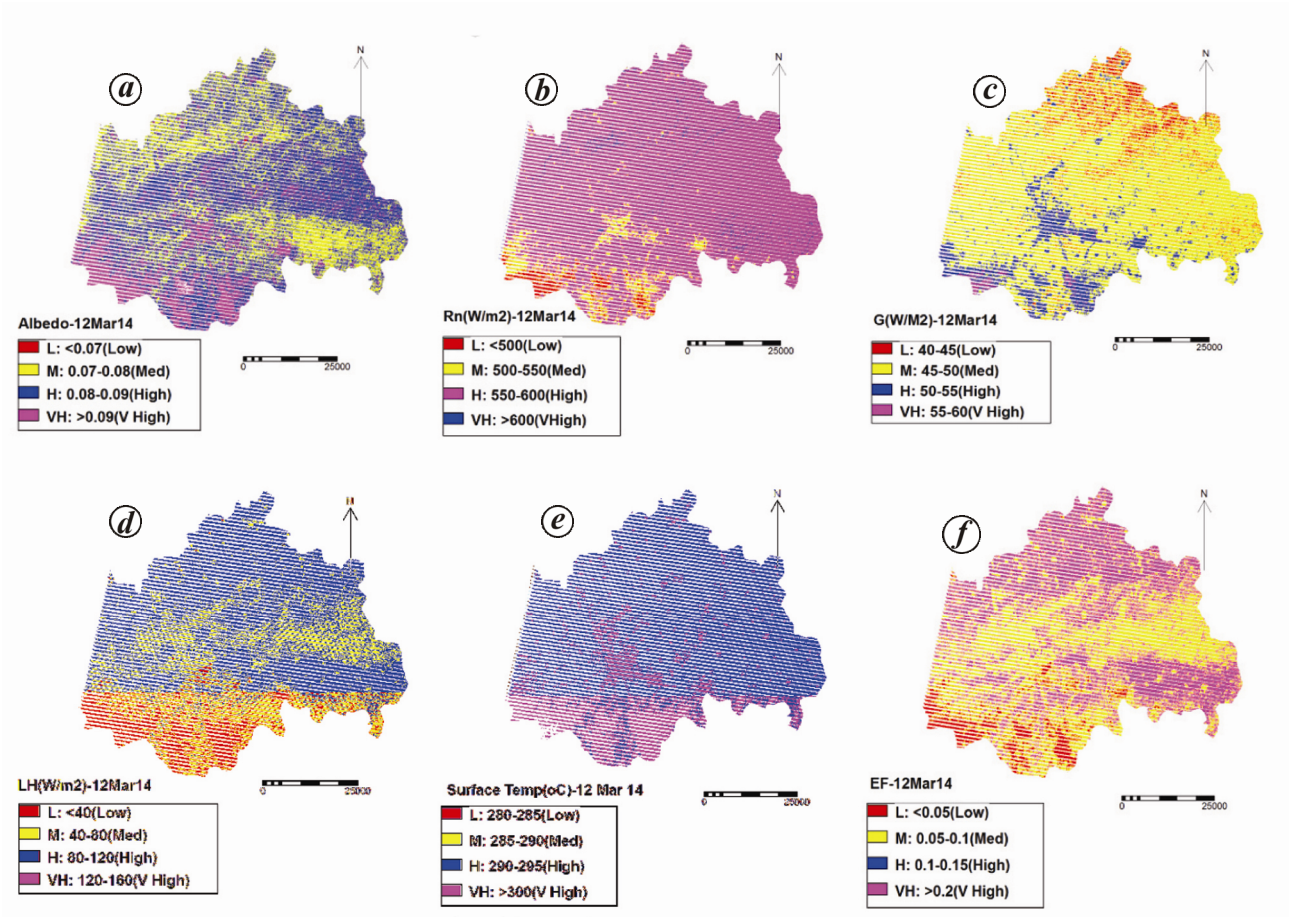

Figure 6. ***a***, Albedo; ***b***, Net radiation; ***c***, Soil heat flux; ***d***, Latent heat flux; ***e***, Surface temperature; ***f***, Evaporative fraction.

availability of energy, and water molecules need minimum energy to leave the surface of water or soil, which can be further enhanced by turbulence and convection. These effects will be more if wind speed is more; hence some days show very high ET values.

ET estimation is essential for hydrological budgeting and decision-making processes related to irrigation scheduling, groundwater recharge and climate change models. By applying lysimeter data validated and PM model validated SEBAL method, spatial ET was estimated for the study area. The following conclusions can be drawn from the study.

SEBAL is one of the best models available to estimate spatial ET. Using the SEBAL model, actual ET can be

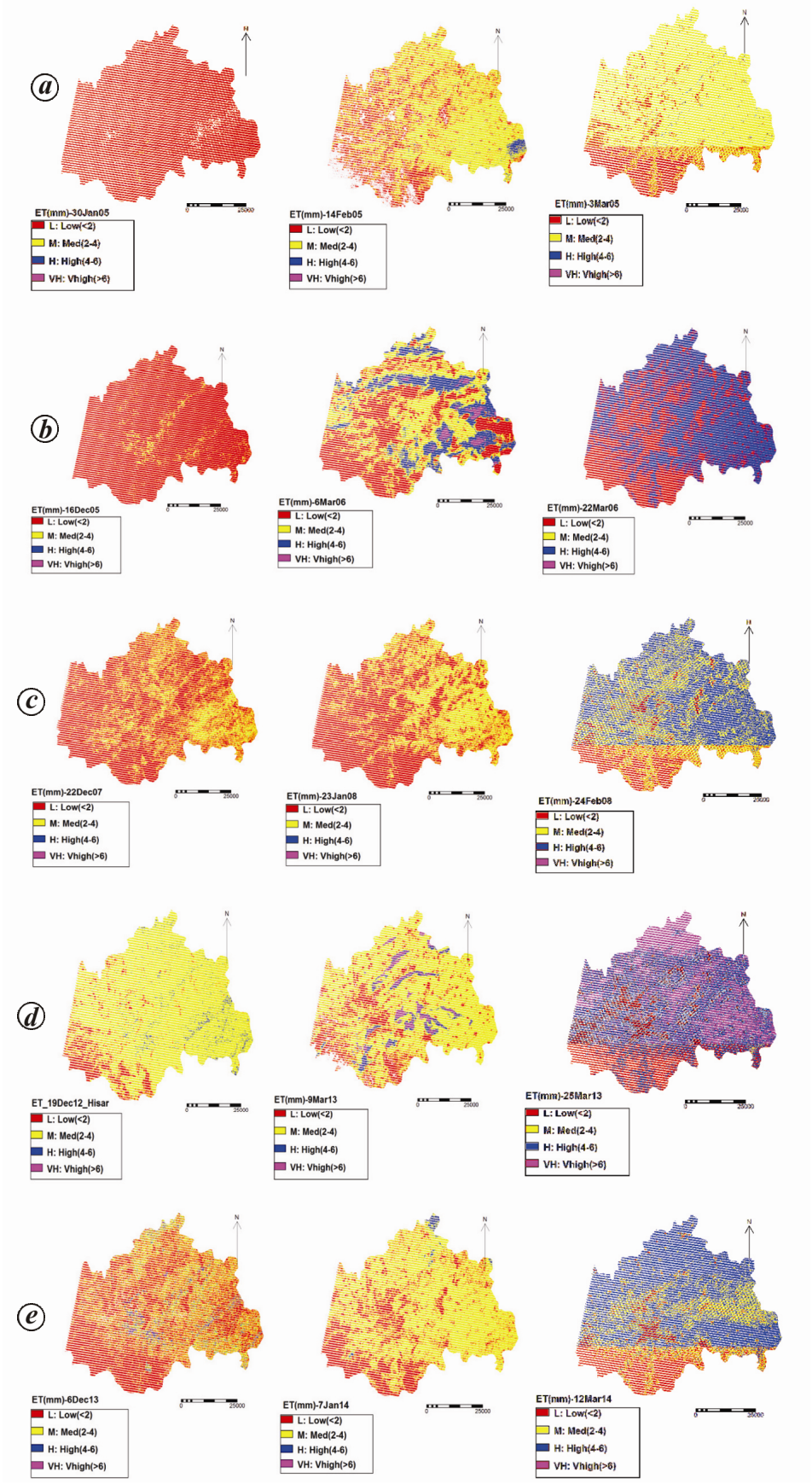

Figure 7. Actual ET for wheat crop season of (***a***) 2004–05; (***b***) 2005–06; (***c***) 2007–08; (***d***) 2012–13; (***e***) 2013–14 in Hisar district.

Table 5. Comparison of values between SEBAL ET and Penman ET

	19 December 2012	9 March 2013	25 March 2013	6 December 2013	7 January 2014	12 March 2014
SEBAL_ET	2.25	3.79	4.07	1.62	2.53	4.09
PM_ET	1.88	3.33	3.13	1.76	2.85	3.26
R^2			0.835			
RMSE			0.583			
NRMSE			0.263			

SEBAL_ET, Crop evapotranspiration by SEBAL model; PM_ET, Crop evapotranspiration by Penman Monteith model/method; RMSE, Root mean square error; NRMSE, Normalized root mean square error.

Table 6. ET_{avg}, ET_{min} and ET_{max} for five wheat crop seasons in the study area

Date	ET_{avg}	ET_{min}	ET_{max}
30 January 2004	1.53	1.29	1.77
14 February 2005	3.25	2.47	3.39
3 March 2005	3.11	2.6	3.36
16 December 2005	1.14	1.12	1.18
6 March 2006	3.51	3.42	6.06
22 March 2006	4.3	4.16	4.3
22 December 2007	1.16	1.12	2.48
23 January 2008	2.2	2.16	2.31
24 February 2008	3.47	3.36	5.29
19 December 2012	2.41	2.25	3.93
9 March 2013	3.79	1.78	3.86
25 March 2013	4.42	1.91	6.78
6 December 2013	1.62	1.61	3.45
7 January 2014	2.53	2.45	2.59
12 March 2014	4.09	2.03	4.16

estimated from satellite images; it does not require any prior knowledge about the crops, their types and cropping seasons. All these make ET estimation more feasible for those working in research disciplines other than agriculture.

The SEBAL model is also capable of estimating spatial ET for composite terrain representing heterogeneous areas, making it a potential tool in the sustainable management of water resources in arid and semi-arid areas with varying geomorphological conditions.

Validation of ET estimation using actual lysimeter data is a robust technique to validate ET at field scale. FAO standardized PM model is also a good method for estimating ET at field scale. It requires extensive dataset for accurate ET estimation. Both these methods were applied to validate ET estimated using SEBAL model. Results show good agreement for actual ET estimation. Use of SEBAL model and Landsat7 ETM+ imagery for ET estimation is a promising method to estimate ET, irrespective of the availability of crop-related information.

The SEBAL model showed variations in average ET values estimated for Hisar district, representing different stages of crop growth. Therefore, it can be used to estimate ET for different stages of crop growth in the study area. This might help in the estimation of crop water requirement, irrigation water management and ultimately as a potential decision-making tool for regional sustainable development.

Actual ET estimated by SEBAL model includes estimation of parameters like LAI, NDVI, albedo and surface temperature and evaporative fraction, thus making it a reliable and feasible technique for ET estimation.

In the present study, validation of SEBAL ET estimation model has been done. Success of RS-based spatial ET estimation depends on the availability of cloud-free RS images. Sometimes cloud-free images also contain line drops resulting into stripes in the images. Thus the SEBAL model is best suited for spatial ET estimation. However, there is scope for sensitivity analysis of the SEBAL model parameters. Also, the model can be validated with various important parameters like temperature, relative humidity and wind speed.

1. Gupta, S. P., India vision 2020. Online document of the Planning Commission, Government of India; http://planningcommission.nic.in/reports/genrep/pl_vsn2020.pdf
2. Bastiaansen, W. G. M., SEBAL-based sensible and latent heat fluxes in the irrigated Gediz Basin, Turkey. *J. Hydrol*., 2000, **229**, 87–100.
3. Roerink, G. J., Su, Z. and Menenti, M., S-SEBI: a simple remote sensing algorithm to estimate thesurface energy balance. *Phys. Chem. Earth*, *Part B*, 2000, **25**,147–157.
4. Kustas, W. P. and Norman, J. M., A two-source approach for estimating turbulent fluxes using multiple angle thermal infrared observations. *Water Resour. Res*., 1997, **33**, 1495–1508.
5. Su, Z., The surface energy balance system (SEBS) for estimation of turbulent heat fluxes. *Hydrol. Earth Syst. Sci.*, 2002, **6**, 85–100.
6. Bastiaansen, W. G. M., Pelgrum, H., Wang, J., Ma, Y., Moreno, J. F., Roerink, G. J. and Vander, W. T., Asurface energy balance algorithm for land (SEBAL): Part 2 Validation. *J. Hydrol*., 1998, **212–213**, 198–212.
7. Bala, A., Rawat, K. S., Misra, A. K. and Srivastava, A., Assessment and validation of evapotranspiration using SEBAL algorithm and Lysimeter data of IARI agricultural farm, India. *Geocarto Int.*, 2015; doi:10.1080/10106049.2015.1076062.
8. Allen, R. G., Pereira, L. S., Raes, D. and Smith, M., Crop ET-guidelines for computing crop water requirements. FAO Irrigation and Drainage Paper 56, Food and Agriculture Organization of the United Nations, Rome, 1998.
9. Peacock, C. E. and Hess, T. M., Estimating evapotranspiration from a reed bed using the Bowen ratio energy balance method. *Hydrol. Process.*, 2004, **18**, 247–260.

10. Lockwood, J. G., Is potential evapotranspiration and its relationship with actual evapotranspiration sensitive to elevated atmospheric CO_2 levels? *Climatic Change*, 1999, **41**, 193–212.
11. Yu, G. R., Wen, X. F., Sun, X. M., Tanner, B. D. and Lee, X. H., Overview of China flux and evaluation of its eddy covariance measurement. *Agric. For. Meteorol.*, 2006, **137**, 125–137.
12. Karimi, P. and Bastiaanssen, W. G. M., Spatial evapotranspiration, rainfall and land use data in water accounting – Part 1: Review of the accuracy of the remote sensing data. *Hydrol. Earth Syst. Sci. Discuss*., 2014, **11**, 1–51.
13. Tasumi, M., Trezza, R., Allen, R. G. and Wright, J. L., Operational aspects of satellite-based energy balance models for irrigated crops in the semi-arid US. *Irrig. Drain. Syst.*, 2005, **19**, 355–376.
14. Liou, Y. A. and Kar, S. K., Evapotranspiration estimation with remote sensing and various surface energy balance algorithms. a review. *Energies*, 2014, **7**, 2821–2849.
15. Saroj Sharma, M. P. and Prawasi, R., Geospatial approach cropping system analysis: a case study of Hisar district in Haryana. *Int. J. Comput. Technol. Appl.*, 2014, **5**, 457–461.
16. Bastiaanssen, W. G. M. and Roebeling, R. A., Analysis of land surface exchange processes in two agricultural regions in Spain using Thematic Mapper Simulator data. In Joint IAHS/IAMAP Symposium, Yokohama, Japan, IAHS, 11–23 July 1993, vol. 212, pp. 407–416.

ACKNOWLEDGEMENTS. We thank the Project Director, Water Technology Centre, Indian Agricultural Research Institute for providing the lysimeter data for validation of the SEBAL model.

Received 24 April 2016; revised accepted 6 February 2017

doi: 10.18520/cs/v113/i01/134-141

Numerical simulation of air-core vortex at intake

Behrouz Khadem Rabe[1,*], Seyyed Hossein Ghoreishi Najafabadi[1] and Hamed Sarkardeh[2]

[1]Department of Water and Environmental Engineering, Shahid Beheshti University, East Vafadar Blvd., Tehranpars, Tehran 167651719, Iran
[2]Department of Civil Engineering, Faculty of Engineering, Hakim Sabzevari University, Tohid Shahr, Sabzevar 9617976487, Iran

In order to study the features of vortex at horizontal intakes, numerical investigations have been performed. The tangential, radial, and axial distributions, and water surface profile were simulated to evaluate the flow behaviour and existence of an air-core vortex. The numerical results agree with existing experimental data. The correlation of vortex characteristics between numerical and experimental results was good. Regarding formed funnel profile of flow in the basin towards horizontal intake, its limits at the existence of an air-core vortex were analysed. The spiral flow pattern from surface towards intake was identified around the air-core vortex. This numerical simulation may help to get a deeper understanding in determining the submergence required to avoid air-entraining vortices in a reservoir.

Keywords: Air-core vortex, flow pattern, numerical simulation, velocity components, water surface profile.

FORMATION of free surface vortex at hydraulic intakes is an undesirable phenomenon. Engineers attempt to avoid formation of vortices in the vicinity of hydraulic facilities, because of severe technical difficulties that may arise. The features and strength of vortices are different and change with circumstances of flow and basin geometry[1]. In order to avoid problems arising from vortex formation at hydraulic intakes, better understanding of its mechanism will be helpful. One significant factor in vortex studies is the intake submergence, S which is defined as the distance between water surface and intake central axis[2]. Vortices are classified based on strength and shape into three different classes by Sarkardeh *et al.*[3].

Rankine[4] offered a mathematical model in which a rotating inner core of solid-body was bound by an outer zone of irrotational vortex motion. All vorticities were limited to the inner core zone and the outer zone was free of vorticity. During the last few decades, different studies experimentally modelled flow field in the presence of vortices to understand the behaviour of this phenomenon[3,5–18]. Besides experimental studies, researchers also tried to numerically simulate vortex formation in the reservoirs[19–27].

Despite such studies, there was no comprehensive numerical study on the characteristics of vortex flow with a strong air-core over a vertical intake. Indeed, in most of the earlier numerical studies, free surface vortex was simulated without air-core and little information was presented on the flow characteristics in a reservoir at the existence of an air-core vortex. This study aims to simulate spiral flow field towards a horizontal intake, analysing a 3D numerical model and verifying the results by experimental data.

Numerical simulation of vortex occurrence and surrounding flow shape in a tank was performed by solving three-dimensional Navier–Stokes equations of fluid motion based on finite volume method (FVM). Turbulence effects were modelled by large eddy simulation (LES) model. Cartesian grid also was used to mesh computational domain. By employing the fraction area/volume obstacle representation (FAVOR) method, walls, bed and vertical intake were defined as obstacles in the flow domain. The free surface was simulated by volume of fluid (VOF) method. Based on VOF method, cells

*For correspondence. (e-mail: b_khadem@sbu.ac.ir)